PCCP

Accepted Manuscript

ROYAL SOCIETY OF CHEMISTRY

www.rsc.org/pccp

Graphical abstract

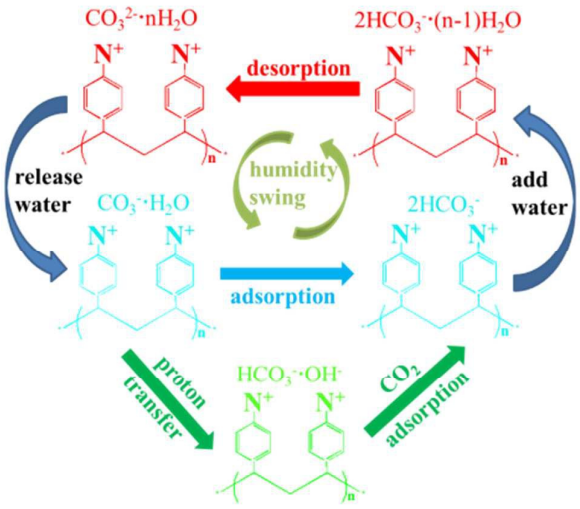

How does a humidity swing adsorption process work? The water at the interface of quaternary ammonium-based polymeric ionic liquids has a great influence on the reaction pathways of CO_2 adsorption, as well as equilibrium of adsorption/desorption (see picture). Theoretical studies are conducted to reveal the underlying mechanisms, especially the proton transfer process of hydrated water.

Journal Name

ARTICLE

Theoretical Studies on CO_2 Capture Behavior of the Quaternary Ammonium-Based Polymeric Ionic Liquids

Received 00th January 20xx,
Accepted 00th January 20xx

DOI: 10.1039/x0xx00000x

www.rsc.org/PCCP

Tao Wang*[a], Kun Ge[a], Kexian Chen[b,c], Chenglong Hou[a], Mengxiang Fang[a]

Quaternary ammonium-based polymeric ionic liquids (PILs) are novel CO_2 sorbent for that they have high capacity, high stability and high binding energy. Moreover, the binding energy of ionic pairs to CO_2 is tunable by changing the hydration state so that the sorbent can be regenerated through humidity adjustment. In this study, theoretical calculations were conducted to reveal the mechanism of the humidity swing CO_2 adsorption, based on model compounds of quaternary ammonium cation and carbonate anions. The electrostatic potential map demonstrates the anion, rather than cation, is chemically preferential for CO_2 adsorption. Further, the proton transfer process from water to carbonate at sorbent interface is successfully depicted with an intermediate which has higher energy state. By determining the CO_2 adsorption energy and activation energy at different hydration state, it is discovered that water could promote CO_2 adsorption by reducing energy barrier of proton transfer. The adsorption/desorption equilibrium would shift to desorption by adding water, which constitutes the theoretical basis for humidity swing. By analyzing the hydrogen bond and structure of water molecules, it is interesting to find that the CO_2 adsorption weakens the hydrophilicity of sorbent and results in release of water. The requirement of latent heat for the phase change of water could significantly reduce the heat of adsorption. The special "self-cooling" effect during gas adsorption can lower the temperature of sorbent and benefit the adsorption isotherms.

1. Introduction

Research and development on novel CO_2 sorbents to mitigate climate change have attracted intense attention recently[1]. Most of the developed solid sorbents have unique interfacial properties, such as porous structures and modifiable functional groups[2, 3]. In this scene, polymeric ionic liquids (PILs) were proposed to capture CO_2 for that they possess characteristics of ionic liquids and macromolecular architecture together[4]. The PILs refer to a special type of polyelectrolytes that carry an ionic liquid species in each of the repeating units[4]. Compared to the corresponding ionic liquid monomers, the CO_2 adsorption capacities of PILs can be several times higher and the sorption-desorption rates can be 10 times faster[5]. PILs also have good thermal stability and anticipated flexibility due to their polymeric nature.

The effects of anion, cation, and backbone of a PIL on its CO_2 adsorption capacity have been studied by different groups[5-11]. For most of the developed PILs with mechanism of physical adsorption, it has been concluded that cations play a major role in determining characteristics of PILs, while anions are more decisive in the case of ionic liquids (ILs)[11]. The CO_2 adsorption capacities of PILs containing different cations have been observed to decrease in the order of ammonium> pyridinium > phosphonium > imidazolium[5-7]. Another type of PILs employs alkaline anions to adsorb CO_2 chemically. Recently, a series of quaternary ammonium-based PILs with exchangeable anions have been developed to capture CO_2. R. Quinn et al.[12] found that PILs containing anions of fluoride or acetate anions could remove carbon dioxide and hydrogen sulfide from gas streams. The sorbent shows a higher CO_2 affinity with decreased degree of anion hydration. By introducing carbonate ion into quaternary ammonium based PILs to form poly[4-vinylbenzyltrimethylammonium carbonate] (P[VBTEA][CO_3^{2-}]), Wang et al.[13] demonstrated that the material has a strong affinity for CO_2 so that it can capture CO_2 at ultra-low concentration (400 ppm). More interestingly, PILs adsorb CO_2 when dry and release CO_2 when wet, which constitutes a humidity swing cycle. He et al.[14-17] synthesized a series of porous polymeric materials containing quaternary ammonium ions and carbonate counter ions to capture CO_2 at 400 ppm. The same characteristics of humidity swing adsorption were observed.

[a] State Key Laboratory of Clean Energy Utilization, Zhejiang University, Hangzhou, 310027, P. R. China. E-mail: oatgnaw@zju.edu.cn
[b] College of Chemical and Biological Engineering, Zhejiang University, Hangzhou, 310027, P. R. China.
[c] College of Food and Biology Engineering, Zhejiang Gongshang University, Hangzhou, 310018, P. R. China

† Electronic Supplementary Information (ESI) available: Fig. S1 shows the optimized structures of model compounds of PILs with different anions and hydrated water molecules, whose steady conformers are shown in Fig. S2, whose atoms in molecules (AIM) analysis is shown in Fig. S3, whose electrostatic potential maps are shown in Fig. S4. Table S1 shows Electron Density (ρ) and Laplacian of the Electron Density ($\nabla^2\rho$) in the BCPs of H-bonds displayed in Fig. S3. Figure S5 shows direct interaction of CO_2 and model compounds of P[VBTEA][CO_3^{2-}]. See DOI: 10.1039/x0xx00000x

The interaction between ions and water could play an important role in the CO_2 adsorption of quaternary ammonium based ILs or PILs. By X-ray crystallography analysis on CO_2 sorbent of tetramethylammonium fluoride tetrahydrate ($[(CH_3)N]F\cdot 4H_2O$), R. Quinn et al.[18] detected strong H-bonds between anions and water which would result in water molecules of enhanced basicity or even free OH^- ions. CO_2 bound as HCO_3^- was observed by nuclear magnetic resonance (NMR) for both ILs and PILs sorbent after CO_2 adsorption.[12, 18] By investigating the CO_2 adsorption isotherms of P[VBTEA][CO_3^{2-}] under different hydration states, Wang et al.[19] observed that the binding energy between CO_2 and PILs increases with decreased number of hydration water. The authors concluded that the dissociation of hydrated water and formation of OH^- should be much more favored with decreased hydration water. However, details of the adsorption process, including the breaking/formation of bonds and energy barrier of elementary steps, are hard to be depicted by current experimental technologies.

Theoretical studies provide an alternative way to reveal the underlying mechanisms of CO_2 adsorption, because it provides relevant information about the microscopic features controlling CO_2 adsorption process[20-23]. Electronic structure methods have proven to be capable of characterizing ionic liquid-CO_2 system, providing valuable information on aspects such as intermolecular hydrogen bonding, charge transfer, structural changes, reaction pathways and the effect of water[24-29]. Lardge et al.[30] simulated the interaction between water and calcite and found that the water could be dissociated near anion vacancies which resulted in a bicarbonate ion and a hydroxide ion. In this study, density functional theory (DFT) is employed to study the underlying mechanism of CO_2 adsorption of P[VBTEA][CO_3^{2-}]. Hydroxide anion, bicarbonate anion and carbonate anion will be studied as the counter ions of quaternary ammonium cation. The structures of ionic pairs are analyzed at the B3LYP/6-311++G** level of theory. The mechanisms of water dissociation, as well as the reaction pathways of CO_2 adsorption are revealed by determining corresponding transition-state (TS) and intermediate (IM). At last, the effects of hydrated water and ionic pairs on adsorption thermodynamics are discussed.

2. Computational methods

Finite oligomer method was employed for computation of electronic structure of PILs.[31, 32] The sorbent material studied in this work is the polymer of P[VBTEA][CO_3^{2-}] whose repeat unit is illustrated in Scheme 1 (a). The quaternary ammonium cation is covalently linked to polystyrene backbone and the counter anion is paired to the cation through ionic bonds. A series material studies on P[VBTEA][CO_3^{2-}][14-17] have shown that the CO_2 adsorption properties are dominated by the ion pairs. Therefore, to reduce the computational cost, the model compounds in this article could be simplified as the ionic pairs of quaternary ammonium cation and counter ions[33], as shown in Scheme 1 (b). To keep the characteristic of solid-state polymer in the model compounds, the distance between the nitrogen-atoms in cations is fixed by freezing the nitrogen-atoms during optimization.

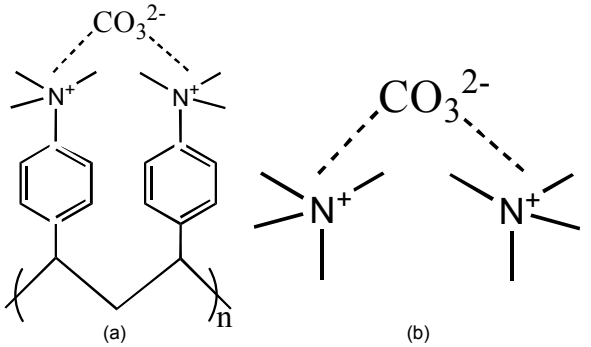

Scheme 1. Chemical structures of repeat unit of P[VBTEA][CO_3^{2-}] (a) and its simplified model compound (b).

All calculations were carried out using the Gaussian 03 package. The DFT method with the Becke's three-parameter functional and the nonlocal correlation of Lee, Yang, and Parr (B3LYP)[34] together with the 6-311++G**[35] basis set were used for all calculations. Previous studies have demonstrated that the DFT method is suitable for calculation of ionic pairs[36-39]. Vibration frequencies were calculated at the same level of theory to confirm the minimum state in potential energy surface (PES). The optimized TS geometries were confirmed to be connected with designated reactants and products by intrinsic reaction coordinate (IRC) calculations. Energy values were corrected by zero-point vibrational energies (ZPE). All energy values were calculated at the same theoretical level, with basis set superposition error (BSSE) corrected through the counterpoise procedure. Natural bond orbital (NBO)[40] charges and electrostatic potential isosurfaces (EPS) were calculated through populational analysis. Atoms in molecules (AIM) analysis were carried out using the AIM2000 program package[41], by which the more detailed information of chemical bonds will be calculated to measure the interaction strength.

3. Results and discussion

3.1 Structures of model compounds of PILs

The optimized structures and properties of the ionic pairs were shown in Fig. 1. The ionic pairs with hydroxide (Reactant I) and carbonate ion (Reactant II) are studied as reactants before CO_2 adsorption, and the ionic pair with bicarbonate ion (Product) is studied as the product after CO_2 adsorption. All the three ionic pairs have symmetric structures. The anion is collinear with its counter cation (as in the case of hydroxide) or coplanar with its counter cation (as in the cases of bicarbonate and carbonate). From the electrostatic potential isosurface showed in Fig. 1, one can note a negative charge concentration over oxygen atom in anions and a positive charge concentration over carbon atom in cations. According to Lewis acid-base theory, CO_2 is some sort of acids and will react with the sites that readily provide electrons[42]. Therefore, the anions, instead of quaternary ammonium cation, should be CO_2 adsorption sites.

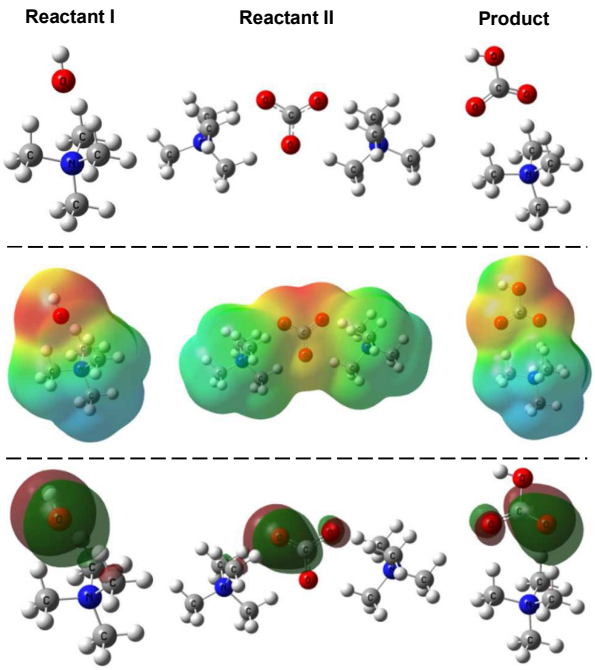

Fig. 1. Schematic representation of the optimized structure, electrostatic potential map and highest occupied molecular orbitals of model compounds of PILs with different anions.

The highest occupied molecular orbitals (HOMO) of ionic pairs further illustrate that the anions are more chemically active and give electrons easily as the HOMO are centered on their anions.

The topological analysis using AIM approach shows the H-bonds formed between oxygen in anions and hydrogen in quaternary ammonium cations (see Fig. 2). According to Bader theory, the values of Electron Density (ρ) and Laplacian of the Electron Density ($\nabla^2\rho$) of bond critical points (BCPs) of H-bonds could fall within the range of 0.002-0.035 and 0.024-0.139 respectively[43]. The values of ρ and $\nabla^2\rho$ in Table 1 are very close to the upper limit, which indicates very strong H-bonds. Interaction energy (ΔE) immediately characterizes the interaction strength and was calculated by the difference between the energy of model compounds and the sum of energy of the corresponding ions. The value of ΔE in Table 1 indicates the interaction between bicarbonate anion and quaternary ammonium cation is the weakest of all. Charge transfer is another parameter to evaluate the anion-cation interaction strength and its values in Table 1 can further support this conclusion.

3.2 Structure of water at PILs interface

The optimized structures of model compounds of PILs with different numbers of hydrated water are shown in Fig. S1. Fig.3 only displays model compounds of PILs with three hydrated water molecules as representatives. PILs with certain number of water molecules would have different conformers, because the molecules are relatively large and relatively weak interactions (such as ionic bond, H-bond) dominate their

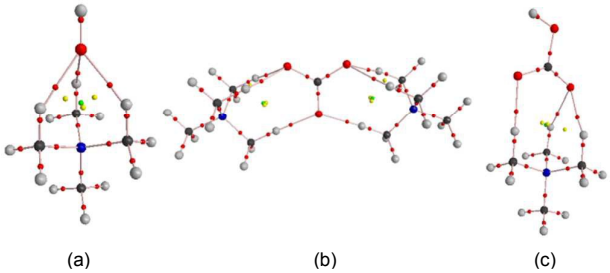

Fig. 2. AIM analysis for optimized structures of model compounds of PILs with (a) hydroxide anion, (b) carbonate anion and (c) bicarbonate anion. Small red dots BCPs, black spheres carbon atoms, gray spheres hydrogen atoms, blue spheres nitrogen atoms, red spheres oxygen atoms, pink lines bond paths.

Table 1. Properties of model compounds of PILs with different anions.

Model compounds	n [a]	ρ [b]	$\nabla^2\rho$ [c]	ΔE [d]	Charge transfer [e]
Hydroxide	3	0.033-0.033	0.112-0.113	49 6	0.118
Carbonate	6	0.032-0.037	0.104-0.111	12 89	0.293
Bicarbonate	3	0.024-0.029	0.080-0.095	39 5	0.040

[a] Number of H-bonds. [b] Electron Density (ρ) of BCPs of H-bonds between anions and cations shown in Fig. 2. [c] Laplacian of the Electron Density (ρ) of BCPs of H-bonds between anions and cations shown in Fig. 2. [d] BSSE corrected interaction energy, kJ/mol. [e] Charge transfer is calculated through the formula: Δq=1-$|q|$, where $|q|$ is the total charge of anion and atomic charges are NPA charges.

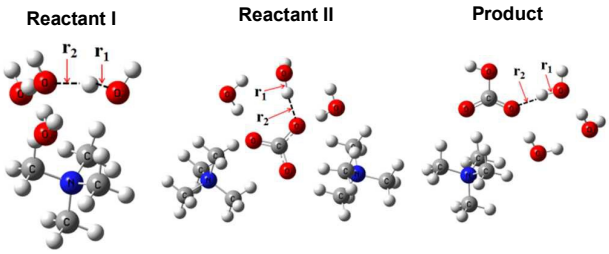

Fig. 3. Optimized structures of model compounds of PILs with different anions and three hydrated water molecules. r_1 is the O-H bond length in the most active hydrated water and r_2 is the length of H-bond.

structures. However, the difference between conformers is small, so is the total energy (less than 2.0 kJ/mol, see Fig. S2). Therefore, we just adopt the most stable ones among their conformers for discussion. The water molecules locate around the anions rather than cations because the oxygen atoms in anions have strong electronegativity and can form H-bonds with water more easily.

First, the hydrated water demonstrates different structure properties for PILs with different anions[44]. The structures of model compounds in Fig. 3 show that for PILs with hydroxide or carbonate anions, the anion is surrounded by water molecules which demonstrates a hydrophilic property of ionic pairs. On the other side, for PIL with bicarbonate anion, water molecules self-associate or form clusters which indicates a hydrophobicity property. Similar phenomenon was also

observed in the ionic liquid systems[45-48]. The spatial distribution difference of water molecules could be due to the difference of H-bonds between water and anions. The bond length data in Table 2 shows that the O-H bond length in the most active hydrated water, r_1, for PIL with bicarbonate is smaller than that for the other two model compounds which indicates a relatively stronger interaction inside water molecules for PIL with bicarbonate. These structure properties can be further confirmed by the AIM analysis which is shown in Fig. S3 and Table S1. Therefore, it can be predicted that water would be released from hydration state to environment within the CO_2 adsorption process due to the change of hydrophilicity. This phenomenon has been observed in CO_2 adsorption by PILs [19].

Second, the hydrated water could play multiple roles in the CO_2 adsorption of PILs. As a result of negative charges transfer from anions to surrounded water, the Lewis basicity of water will increase so that new adsorption sites can be formed by the water molecules[18]. The electrostatic potential maps of model compounds (see Fig. S4) have proved that oxygen atom in water becomes another center of negative charge. As shown in Table 2, the relative increment of electronegativity of oxygen-atom in water could be as much as 12.48% compared with that of free water. Moreover, with the increase of interaction between anion and water, new adsorption sites of OH^- could be produced through proton transfer from water to anion[30, 49]. Generally, the H-bond can be regarded as the incipient stage of a proton transfer process[50] and proton displacement could be a measurement of the feasibility of proton transfer[51]. Table 2 shows that the O-H bond lengths in water are all larger than that of free water. The r_1 in model compound with hydroxide or carbonate increases with decreased number of water molecules, while r_2, the length of H-bond decreases with decreased number of water molecules, which indicate a trend of proton transfer with decreased hydration number. The data of atomic charge and bond length in Table 2 also indicates that redundant water molecules in model compounds may distract the negative charges transferred from the anion to water and result in the decrease of basicity of water. As the model compound of PILs with carbonate represents reactant sorbent before CO_2 adsorption, the mechanisms revealed above could explain the observation of decreased CO_2 capacity with increased hydration number or humidity during isotherm experiments[13].

On the other side, model compounds with bicarbonate show a non-monotonic relationship between atomic charge, bond length and the number of water molecules. This is the result of the clusters distribution of hydrated water, which would lead to additional strong interactions among water molecules. When the number of water molecules increases from two to three, the electronegativity of hydrated water and O-H bond length increases while the H-bond length decreases. Meanwhile, the hydrogen atom in water is closer to bicarbonate anion, which is beneficial to the formation of carbonic acid (H_2CO_3). It seems that the increase of water molecules could promote desorption process, which is consistent with the humidity swing process of this PIL material.

3.3 Effects of hydrated water on CO_2 adsorption reactions

3.3.1 PILs with hydroxide anion

Figure 4 is the variation of potential energy with the distance between CO_2 molecule and hydroxide anion, which shows no transition-state during the reaction. When CO_2 molecule attacks the hydroxide anion, a bicarbonate anion will be formed immediately, which indicates a chemical reaction without energy barrier. In the final product of bicarbonate anion, a stable covalent bond (ρ=0.2491, $\nabla^2\rho$=-0.5178 in AIM analysis)[43] is formed between CO_2 molecule and hydroxide anion. The analysis of ion pairs indicates that the hydroxide anion is very active and has a strong electron donating ability. And CO_2 adsorption by model compounds of PILs with hydroxide anion is irreversible. The adsorption energy is calculated as 85.12 kJ/mol.

Table 2. Properties of hydrated water in model compounds of PILs with different anions.

Model compounds	n [a]	Atomic charge [b]	r_1 (Å) [c]	r_2 (Å) [d]
Hydroxide	1	-1.027	1.021	1.595
	2	-1.024	1.018	1.607
	3	-1.016	1.012	1.623
Carbonate	1	-1.012	1.001	1.647
	2	-1.004	0.999	1.665
	3	-1.001	0.996	1.684
Bicarbonate	1	-1.004	0.992	1.693
	2	-1.001	0.981	1.793
	3	-1.013	0.990	1.717

[a] Number of H-bonds. [b] Atomic NBO charge of oxygen-atom in hydrated water. For the case of more than one hydrated water molecule, the atomic charge is the maximum value among them. The atomic NBO charge of oxygen-atom in free water is -0.913. [c] O-H bond length in the most active hydrated water shown in Fig. S1 and Fig. 3. The O-H bond length in free water is 0.962 Å. [d] The length of H-bond of the most active hydrated water shown in Fig. S1 and Fig. 3.

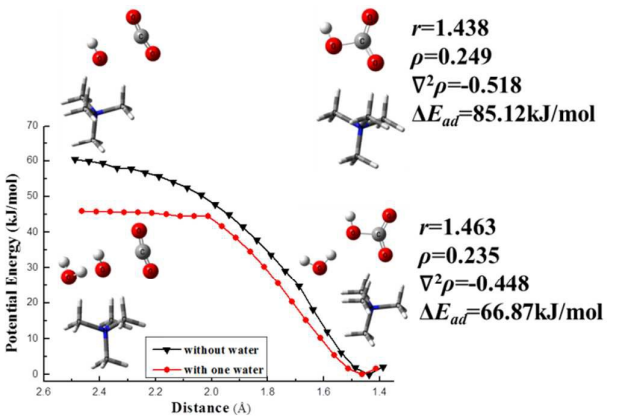

Fig. 4. The variation of potential energy with the distance between CO_2 molecule and hydroxide anion. The energy of stable ionic pairs with bicarbonate anion (whose structures are shown in the right of the figure) is the reference to calculate the potential energy of other structures.

When one water molecule is involved in the CO_2 adsorption reaction, Fig. 4 shows that CO_2 molecule can still react with hydroxide anion and transform into bicarbonate anion without energy barrier. The potential energy curve with hydrated water is below that without water, which indicates the water reduces the interactions between CO_2 molecule and hydroxide anion. This is because parts of negative charges of hydroxide anion have transferred into water. The covalent bond (ρ=0.2352, $\nabla^2\rho$=-0.4476 in AIM analysis) gets weaker compared with the situation without water, and the adsorption energy decreases by 18.25 kJ/mol. Besides, the potential energy has a mild increase when the distance between CO2 and hydroxide anion changes from 2.0 to 2.5 Å, which indicates the bonded term is out of action and the nobonded term takes over as the dominating interactions.

3.3.2 PILs with carbonate anion

The structure analysis on ionic pairs in Sections 3.1 and 3.2 indicates that, for quaternary ammonium-based PILs, the anions are preferential CO_2 adsorption sites. At the same time, the dissociation of water is preferred as the number of water surrounded carbonate ion decreases. Therefore, the interaction between CO_2 and PILs with carbonate anion could consist of the following elementary steps which are similar as those in carbonate solution[52]:

$$CO_2+H_2O\leftrightarrow HCO_3^-+H^+ \quad (1)$$

$$H_2O\leftrightarrow OH^-+H^+ \quad (2)$$

$$CO_2+OH^-\leftrightarrow HCO_3^- \quad (3)$$

$$CO_3^{2-}+H^+\leftrightarrow HCO_3^- \quad (4)$$

The possible reaction paths of CO_2 adsorption on PILs with hydrated carbonate anion are elaborated in Scheme 2. The product of bicarbonate anion could be formed by either reaction path A (Equation (1) and (4)) or reaction path B (Equation (2), (3) and (4)). The activation energy for reaction (1) is generally quite high (e.g. 179.83 kJ/mol[53]), since it involves bending a stable, linear CO_2 molecule (with a water parked oxygen-down over the carbon) into a Y-shaped $O=C(OH)_2$ molecule. The reaction path B could be considered as the process of proton transfer from water to carbonate ion (Equation (2) and (3))[18, 30] with a following reaction between CO_2 and hydroxide anion (Equation (4)). The activation energy for proton transfer is calculated as the energy difference between reactant complexes (RC) and transition-state, as shown in Fig. 5. The activation energy is calculated as 34.66 kJ/mol of CO_2. As studied in Section 3.3.1, the Equation (3) could happen without any energy barrier. Therefore the total activation energy of reaction path B is far smaller than that of pathway A, which indicates the most favorable reaction channel of path B.

Fig. 5 shows that a stable IM with high energy is formed during the proton transfer process. Compared with the energy of TS, the energy of IM is 4.73 kJ lower, which means that the IM has high reaction activity. When CO_2 molecule attacks the hydroxide anion in the IM model compounds, it could transform into bicarbonate without any energy barriers. The

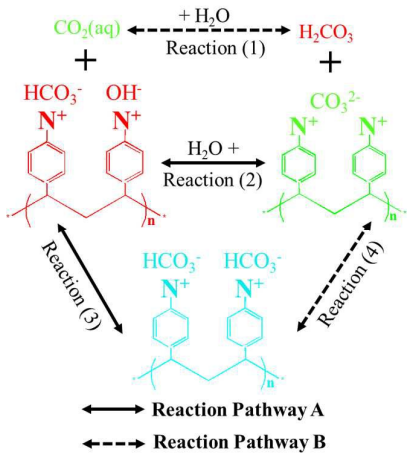

Scheme 2. Schematic diagram of CO_2 adsorption process of PILs with carbonate anion. The solid arrows and dashed arrows represent the two possible reaction pathways respectively. The letters in green represent the initial states of reactants. The letters in red represent the intermediates. The letters in blue represent the final states of products.

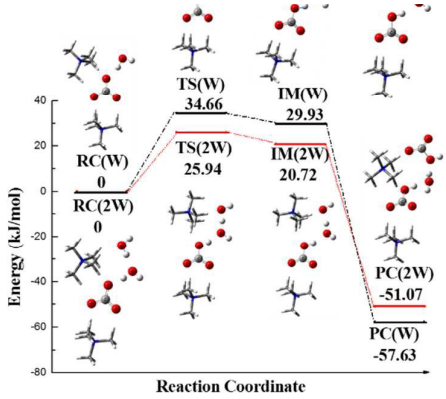

Fig. 5. Optimized reaction geometries and corresponding potential energy profiles for CO_2 adsorption by model compounds of P[VBTEA][CO_3^{2-}] one (W) or two (2W) hydrated water molecules. The energy levels are plotted relative to the separated reactants: model compounds of P[VBTEA][CO_3^{2-}] and one hydrated water molecule plus CO_2 for (W) case, model compounds of P[VBTEA][CO_3^{2-}] and two hydrated water molecules plus CO_2 for (2W) case.

activation energies of adsorption and desorption could also be significantly affected by the hydrated state. As shown in potential energy profiles in Fig. 5, the energy of TS and IM, as well as the energy barrier from product to IM, decrease as one more water molecule is added to the reaction path. Thus, water could promote the reaction kinetics of both the adsorption and desorption as a catalyst. Early in 1983, Williams et al.[54] found that the energy barrier of proton transfer could decrease with assistance of water molecule. The hydrated water would receive transferred proton from surrounded water molecule, and give proton to carbonate anion at the same time[55]. Fig. 5 also shows that the energy difference between reactant and product declines as one more water is involved which could result in the shift of adsorption/desorption equilibrium to desorption. The multiple mechanisms of effect of water constitute the theoretical basis of humidity swing adsorption. At the same time, an optimized

hydration sate (through humidity or hydrophilicity adjustment) would be suggested to seek for the balance of adsorption kinetics and adsorption thermodynamics.

The direct physically interaction between CO_2 and model compounds of P[VBTEA][CO_3^{2-}] without water is also analyzed. The values of ρ and $\nabla^2\rho$ in AIM analysis of BCPs of the bond between CO_2 and carbonate anion are shown in Fig. S5. Compared to the chemical adsorption energy of P[VBTEA][CO_3^{2-}] with one water (57.63 kJ/mol as shown in Fig. 5) and according to the thermodynamic analysis on CO_2 capture[19], the physical adsorption energy of P[VBTEA][CO_3^{2-}] (27.52 kJ/mol) should be too weak to adsorb CO_2 efficiently, especially at ultra-low CO_2 partial pressure.

3.3.3 Water equilibrium and effect on adsorption heat

Previous thermodynamic study has revealed that certain amounts of hydrated water will be released out during CO_2 adsorption for P[VBTEA][CO_3^{2-}] sorbent[19], the equilibrium of water adsorption coupled with CO_2 adsorption could be expressed as the following:

$$[N^+CO_3^{2-}N^+]\cdot aH_2O^{(h)}+CO_2\rightarrow[2N^+HCO_3^-]\cdot bH_2O^{(h)}+(a\text{-}b\text{-}1)H_2O^{(g)} \quad (5)$$

where N^+ represents the fixed cation, $H_2O^{(h)}$ represents the hydrated water, $H_2O^{(g)}$ represents the gaseous water, *a* and *b* represent the number of water around carbonate and bicarbonate anions respectively at certain temperature and partial pressure of water vapor. Since the gas adsorption process is generally exothermic and the water evaporation process is endothermic, the phase change of H_2O from hydrated to gaseous during CO_2 adsorption could lower the apparent heat of adsorption, as well as the temperature of sorbent. As discussed in Section 3.2, the release of water during CO_2 adsorption should be driven by the decreased hydrophilicity of PIL sorbent when the anion is converted from carbonate to bicarbonate. The affinity of water for different types of anion at different hydration state can be calculated (Fig. 6) and the values can be further used to determine the standard state enthalpy change and standard state free energy

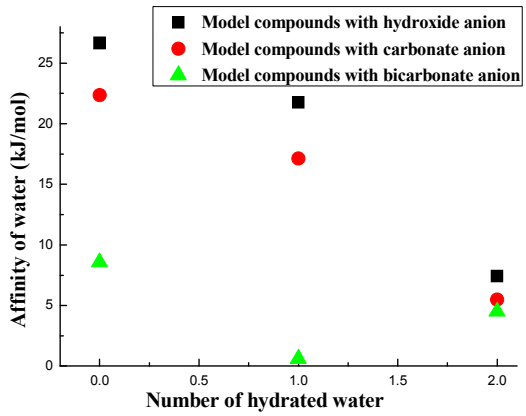

Fig. 6. Calculated affinity of water to model compounds of PILs with various anions studied as a function of number of hydrated water.

Table 3. Thermodynamic parameters of Equation 5 with possible number of hydrated water molecules.

Possible coefficient of Equation (5)		Corresponding thermodynamic parameters	
a	*b*	$\Delta G^{\ominus}$ (kJ/mol)	$\Delta H^{\ominus}$ (kJ/mol)
1	0	-16.724	-17.250
	1	-25.284	-66.110
2	1	-6.170	-7.404
	2	-12.471	-56.264
3	2	-8.270	-7.404
	3	-14.624	-48.677

change of Equation (5). As shown in Table 3, for sorbent with same coefficient *a*, the heat of reaction will dramatically decrease when one more water is released from the product. For chemical adsorption technology, the sorbent generally has high selectivity but high heat of adsorption. The released heat during adsorption is hard to be dissipated in tight packed solid sorbent and would cause the increase of sorbent temperature. Therefore, by designing material with significant difference of hydrophilicity between states before and after adsorption, an interesting "self-cooling" effect could be obtained during adsorption which can benefit the adsorption isotherms.

Conclusions

In this contribution, theoretical studies were performed at the B3LYP/6-311++G** levels of theory to study structures of a carbonate-functionalized quaternary-ammonium-based PILs called P[VBTEA][CO_3^{2-}], its underlying CO_2 adsorption mechanism and the effect of hydrated water. The results showed strong interactions between the ions involved, which could attribute to the strong intermolecular H-bonds between all the studied model compounds. The anions, instead of quaternary ammonium cation, are CO_2 adsorption sites for their ability to provide electrons. The hydrated water could affect the structures and electronic properties of model compounds through H-bonds formed between them. The hydrated water shows the tendency of proton transfer to form hydroxide in model compound of carbonate, while shows the tendency of forming carbonic acid in model compound of bicarbonate. The mechanism of CO_2 adsorption was confirmed by calculating the activation energy of possible reaction pathways. An IM with high energy and reaction activity should be achieved before adsorbing CO_2. The hydrated water could promote CO_2 adsorption by reducing the energy of transition state as well as change the adsorption/desorption equilibrium through increasing the energy of product. From the thermodynamic point of view, the differences of affinity of water between model compounds of PILs with different anions could be regarded as the theoretical basis for their unique characteristics, such as low reaction enthalpy and humidity swing.

Acknowledgements

This study is supported by the National Natural Science Foundation (No.51306161), the Natural Science Foundation of Zhejiang Province, China (No. LY13E060004), the Specialized Research Fund for the Doctoral Program of Higher Education of China (No. 20130101120143) and the fundamental research funds for the central universities.

Notes and references

1 J. Wang, L. Huang, R. Yang, Z. Zhang, J. Wu, Y. Gao, Q. Wang, D. O'Hare, Z. Zhong, *Energy Environ. Sci.* **2014**, 7, 3478–3518.
2 J. Wang, H. Huang, M. Wang, L. Yao, W. Qiao, D. Long, L. Ling, *Ind. Eng. Chem. Res.* **2015**, 54, 5319−5327.
3 C. F. Cogswell, H. Jiang, J. Ramberger, D. Accetta, R. J. Willey, S. Choi, *Langmuir* **2015**, 31, 4534−4541.
4 J. Yuan, M. Antonietti, *Polymer* **2011**, 52, 1469-1482.
5 J. Tang, H. Tang, W. Sun, M. Radosz, Y. Shen, *Polymer* **2005**, 46, 12460–12467.
6 J. Tang, H. Tang, W. Sun, M. Radosz, Y. Shen, *J. Polym. Sci., Part A: Polym. Chem.* **2005**, 43, 5477–5489.
7 J. Tang, H. Tang, W. Sun, H. Plancher, M. Radosz, Y. Shen, *Chem. Commun.* **2005**, 26, 3325–3327.
8 A. Blasig, J. Tang, X. Hu, Y. Shen, M. Radosz, *Fluid Phase Equilib.* **2007**, 256, 75–80.
9 P. G. Mineo, L. Livoti, M. Giannetto, A. Gulino, S. L. Schiavo, P. Cardiano, *J. Mater. Chem.* **2009**, 19, 8861–8870.
10 P. G. Mineo, L Livoti, S. L. Schiavo, P. Cardiano, *Polym. Adv. Technol.* **2012**, 23, 1511–1519.
11 W Fang, Z. Luo, J. Jiang, **2013**, 15, 651-658.
12 R. Quinn, *Sep. Sci. Technol.* **2003**, 38, 3385–3407.
13 T. Wang, K. S. Lackner, A. Wright, *Environ. Sci. Technol*. **2011**, 45, 6670–6675.
14 H. He, M. Zhong, D. Konkolewicz, K. Yacatto, T. Rappold, G. Sugar, N. E. David, K. Matyjaszewski, *J. Mater. Chem. A* **2013**, 1, 6810-6821.
15 H. He, W. Li, M. Lamson, M. Zhong, D. Konkolewicz, C. Hui, K. Yaccato, T. Rappold, G. Sugar, N. E. David, K. Damodaran, S. Natesakhawat, H. Nulwala, K. Matyjaszewski, *Polymer* **2014**, 55, 385-394.
16 H. He, W. Li, M. Zhong, D. Konkolewicz, D. Wu, K. Yaccato, T. Rappold, G. Sugar, N. E. David, K. Matyjaszewski, *Energy Environ. Sci.* **2013**, 6, 488-493.
17 H. He, W. Li, D. Konkolewicz, K. Yaccato, T. Rappold, G. Sugar, N. E. David, J. Gelb, N. Kotwal, A. Merkle, K. Matyjaszewski, *Adv. Funct. Mater.* **2013**, 23, 4720–4728.
18 R. Quinn, J. B. Appleby, G. P. Pez, *J. Am. Chem. Soc.* **1995**, 117, 329-335.
19 T. Wang, K. S. Lackner, A. Wright, *Phys. Chem. Chem. Phys.* **2013**, 15, 504-514.
20 X. Zhang, F. Huo, Z. Liu, W. Wang, W. Shi, E. J. Maginn, *J. Phys. Chem. B* **2009**, 113, 7591–7598.
21 M. E. Perez-Blanco, E. J. Maginn, *J. Phys. Chem. B* **2011**, 115, 10488–10499.
22 L. X. Dang, T. M. Chang, *J. Phys. Chem. Lett.* **2012**, 3, 175–181.
23 O. Hollóczki, Z. Kelemen, L. Könczöl, D. Szieberth, L. Nyulászi, A. Stark, B. Kirchner, *ChemPhysChem.* **2013**, 14, 315–320.
24 B. E. Gurkan, J. C. D. L. Fuente, E. M. Mindrup, L. E. Ficke, B. F. Goodrich, E. A. Price, W. F. Schneider, J. F. Brennecke, *J. Am. Chem. Soc.* **2010**, 132, 2116–2117.
25 M. I. Cabaco, M. Besnard, Y. Danten, J. A. P. Coutinho, *J. Phys. Chem. B* **2011**, 115, 3538–3550.
26 C. Wu, T. P. Senftle, W. F. Schneider, *Phys. Chem. Chem. Phys.* **2012**, 14, 13163–13170.
27 J. Chen, W. Li, X. Li, H. Yu, *Phys. Chem. Chem. Phys.* **2012**, 14, 4589–4596.
28 S. Aparicio, M. Atilhan, *J. Phys. Chem. B* **2012**, 116, 9171–9185.
29 I. Khan, K. A. Kurnia, F. Mutelet, S. P. Pinho, J. A. P. Coutinho, *J. Phys. Chem. B* **2014**, 118, 1848−1860.
30 J. S. Lardge, D. M. Duffy, M. J. Gillan, M. Watkins, *J. Phys. Chem. C* **2010,** 114, 2664-2668.
31 S. Motaghiani, K. Mirabbaszadeh, *Int. J. Quantum Chem* **2013**, 113, 1650–1659.
32 J. Torras, J. Casanovas, C. Alemán, *J. Phys. Chem. A* **2012**, 116, 7571-7583.
33 Y. Zhao, Y. Choe, E. Tsuchida, E. Ikeshoji, A. Ohira, *J. Phys. Chem. C* **2015**, 119, 11362−11369.
34 A. D. Becke, *J. Chem. Phys.* **1993**, 98, 5648−5652.
35 R. Ditchfield, W. J. Hehre1, J. A. Pople, *J. Chem. Phys.* **1971**, 54, 724−728.
36 B. L. Bhargava, S. Balasubramanian, *Chem. Phys. Lett.* **2007**, 444, 242−246.
37 C. Lagrost, S. Gmouh, M. Vaultier, P. Hapiot, *J. Phys. Chem. A* **2004**, 108, 6175−6182.
38 E. R. Talaty, S. Raja, V. J. Storhaug, A. Dölle, W. R. Carper, *J. Phys. Chem. B* **2004**, 108, 13177−13184.
39 G. Yu, S. Zhang, X. Yao, J. Zhang, K. Dong, W. Dai, R. Mori, *Ind. Eng. Chem. Res.* **2006**, 45, 2875−2880.
40 A. E. Reed, L. A. Curtiss, F. Weinhold, *Chem. Rev.* **1998**, 88, 899–926.
41 F. Biegler-König, J. Schönbohm, D. Bayles, *J. Comput. Chem.* **2001**, 22, 545–559.
42 L. J. Murphy, K. N. Robertson, R. A. Kemp, H. M. Tuononen, J. A. C. Clyburne, *Chem. Commun.* **2015**, 51, 3942-3956.
43 S. J. Grabowski, *J. Mol. Struct.* **2001**, 562, 137-143.
44 J. E. S. J. Reid, A. J. Walker, S. Shimizu, *Phys. Chem. Chem. Phys.* **2015**, 17, 14710-14718.
45 Y. Dantena, M. I. Cabaço, M. Besnard, *J. Mol. Liq.* **2010**, 153, 57–66.
46 X. Zhu, Y. Wang, H. Li, *AIChE J.* **2009**, 55, 198–205.
47 A. Dominguez-Vidal, N. Kaun, M. J. Ayora-Cañada, B. Lendl, *J. Phys. Chem. B* **2007**, 111, 4446–4452.
48 A. Maiti, A. Kumar, R. D. Rogers, *Phys. Chem. Chem. Phys.* **2012**, 14, 5139-5146.
49 D. J. Dai, S. J. Peters, G. E. Ewing, *J. Phys. Chem.* **1995**, 99, 10299–10304.
50 H. B. Buergi, J. D. Dunitz, *Acc. Chem. Res.* **1983**, 16, 153–161.
51 A. N. Isaev, *Russ. J. Phys. Chem. A* **2012**, 86, 69–74.
52 A. H. G. Cents, D. W. F. Brilman, G. F. Versteeg, *Chem. Eng. Sci.* **2005**, 60, 5830–5835.
53 P. P. Kumar, A. G. Kalinichev, R. J. Kirkpatrick, *J. Chem. Phys.* **2007**, 126, 204315.
54 I. H. Williams, D. Spangler, D. A. Femec, G. M. Maggiora, R. L. Schowen, *J. Am. Chem. Soc.* **1983**, 105, 31-40.
55 X. Hu, H. Li, W. Liang, S. Han, *J. Phys. Chem. B* **2005**, 109, 5935–5944